Mixed integration method for the evaluation of the reaction integrals using the spectral domain method

D.Pilz and W.Menzel

Abstract: The spectral domain approach is frequently used for the full-wave analysis of planar structures. Applying Galerkin's method, infinite, double integrals have to be solved. The paper deals with an effective algorithm for solving these integrals using a mixed integration method.

1 Introduction

The spectral domain method (SDM) algorithm is widely used for the analysis of planar microwave circuits, transmission line characteristics and antennas. The electromagnetic fields and currents in one or more layers are transformed from the space domain via Fourier transformation into the spectral domain. Thus the convolutional integrals of the space domain are transformed into simple multiplications in the spectral domain. Additionally, the Green's functions describing the relation between the electromagnetic fields and the related electric or magnetic current, can easily be obtained by using the immittance approach [1].

In the spectral domain approach the unknown currents are usually expanded in a series of known basis functions with unknown coefficients. The scalar product of the test and basis functions, together with the Green's function used in this procedure, leads to two-dimensional integrals, here designated as reaction integrals. In a shielded or periodic structure, the integral can be reduced to a two-dimensional sum using Floquet's theorem. However, in an open structure the two-dimensional infinite integrals including one or more pole rings have to be solved numerically. For the case of small distances between different cells of test and basis functions, this can be done by a simple numerical quadrature in polar co-ordinates [2]. To improve the numerical efficiency the asymptotic behaviour of the integrand for greater spectral co-ordinates can be used to evaluate the outer part of the integral analytically [3–5].

However, if the origins of the test and basis functions are not located close to each other, the integrals show a highly oscillating behaviour. This leads to severe difficulties in finding an accurate solution. This holds especially for the subdomain basis function or larger antenna arrays, where numerous equivalent integrals have to be solved.

The spatial integral equation technique may be used for this type of problem, but then the Green's functions have to be determined in the space domain, and several convolution integrals have to be solved [4].

IEE Proceedings online no. 19990630

DOI: 10.1049/ip-map:19990630

Paper first received 6th March and in revised form 14th September 1998

The authors are with the Department of Microwave Techniques, University of Ulm, Albert-Ginstein Allee 41, D–89069, Ulm, Germany

In this paper, a mixed integration method for an efficient algorithm for solving the reaction integral in the spectral domain is presented. The integrand is partly evaluated in Cartesian co-ordinates, wherever possible. After a proper interpolation for the Green's function and a separation in the x- and and y-directions of the current functions, the highly oscillating part is integrated by Filon's method [6]. This leads to a drastic improvement in the convergence, as it will be shown in the results. The remaining part of the integral, the part close to the ring of surface wave poles, is evaluated in a conventional way using the residual theorem.

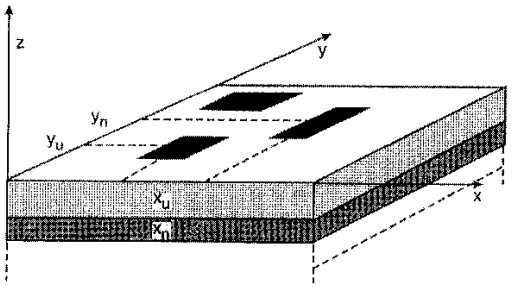

Fig.1 *Configuration of structure under investigation*

2 The standard spectral domain approach

The structure under investigation is shown in Fig. 1. For a planar, infinite structure the related electric fields in the spectral domain are obtained as

$$\overleftrightarrow{G}_J \cdot \vec{J} + \overleftrightarrow{G}_M \cdot \vec{M} = \vec{E}_{tot} - \vec{E}_{inc} \qquad (1)$$

$\overleftrightarrow{G}_J$ and $\overleftrightarrow{G}$M are dyadic Green's function, $\vec{J}$ and $\vec{M}$ are the electric and magnetic currents, $\vec{E}_{tot}$ and $\vec{E}_{inc}$ are the total and the incident electric fields, respectively. For simplification, only electric currents in the y-direction are considered here. Then eqn. 1 reduces to

$$Z_{yy} \cdot J_y = E_{tot,y} - E_{inc,y} \qquad (2)$$

The next step is to expand J_y in a series of basis functions

$$J_y = \sum_{n=1}^{N} c_n \psi_n \qquad (3)$$

The application of Galerkin's procedure with respect to eqn. 2 leads to an inhomogenous matrix equation for the unknown coefficients c_n

$$\overleftrightarrow{A}\vec{c} = \vec{b} \tag{4}$$

The elements in the matrix, the reaction integrals, can be written as

$$A_{un} = \int_{-\infty}^{\infty}\int Z_{yy}\psi_u^*\psi_n dk_x dk_y \tag{5}$$

$$= \int_0^{2\pi}\int_0^{\infty} Z_{yy}\psi_u^*\psi_n k_r dk_r dk_\varphi \tag{6}$$

using the identities $k_r = \sqrt{(k_x^2 + k_y^2)}$ and $k_\varphi = \arctan(k_y/k_x)$; k_r and k_φ are wavenumbers in polar co-ordinates. ψ can be decomposed into one term ϕ, including the shape of the current densities only, and another term, which includes the spacing between the origins of the expansion functions, $\exp\{j(k_x\Delta x + k_y\Delta y)\}$. Eqn. 7 summarises the entire integral

$$A_{un} = \int_{-\infty}^{\infty}\int Z_{yy}\phi_u^*\phi_n e^{j(k_x\Delta x + k_y\Delta y)} dk_x dk_y \tag{7}$$

where the term Z_{yy}, includes the surface wave poles and can be separated into k_r and k_ϕ. The term $\phi_u^*\phi_n$ can be separated into k_x and k_y, and the exponential term is highly oscillating for increasing Δx, Δy.

3 Typical characteristics of the integrand

3.1 Green's function

The integrand is a product of two different types of functions. Using the immittance approach [1], the Green's function Z_{yy} is derived by separating electromagnetic fields and currents into TM_z and TE_z components. The respective Green's functions Z_e and Z_h then have the general form

$$Z_{e,h} = \frac{s_{e,h}(k_{z,i})}{p_{e,h}(k_{z,i})} = f(k_r) \tag{8}$$

where $k_{zi} = \sqrt{(k_r^2 - \varepsilon_{r,i}k_0^2)}$ is the wavenumber in the z-direction in the ith layer, and k_r is the spectral domain which varies in the radial direction. The function p_e contains at least one zero, representing the surface wave pole. All zeros are located in the range $k_0 < k_r < k_0\sqrt{\varepsilon_n}$, where $\sqrt{\varepsilon_n}$ is the largest dielectric constant. Fig. 2 shows a typical example for Z_h and Z_e of a single layer grounded substrate.

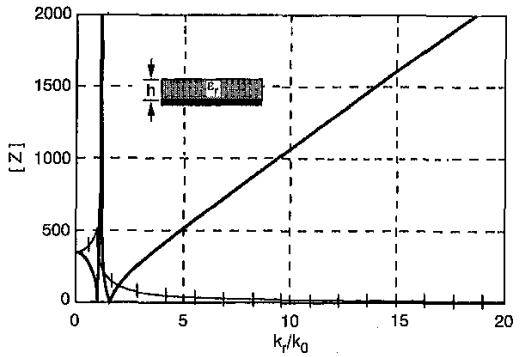

Fig.2 *Absolute values of Green's function for TM_z- and TE_z-waves for a single substrate with ground metallisation*
$h = \lambda/6$, $\varepsilon_r = 2.5$
——— Z_e
++++ Z_h

The relationship between y-directed currents and electric fields can be expressed as

$$Z_{yy} = -\cos(k_\varphi)Z_h(k_r) + \sin(k_\varphi)Z_e(k_r) = f(k_r, k_\varphi) \tag{9}$$

Hence, Z_{yy} is a function, which can be decomposed into the sum of two products each separable in polar co-ordinates. However, a separation in Cartesian co-ordinates is not possible.

3.2 Basis functions

The second term of eqn. 7 consists of the product of a test and a basis function without the representation of the distance between the origins of the two functions. A large group of basis functions is composed of the product of two independent one-dimensional functions, which separately describe the dependencies of the x- and y-directions. In the case of subdomain functions, these are for example the rooftop functions or other derivatives of B-splines or the pentahedral functions [4]. A similar decomposition can be found for entire domain functions for dipoles, crosses, square loops or Jerusalem crosses. These can be written as

$$\phi_u(k_x, k_y) = \phi_{ux}(k_x)\phi_{uy}(k_y) \tag{10}$$

The Fourier transform of the current distributions always extends to infinity as the distribution in the space domain is limited. The behaviour of the transform is determined by the specific form of the current distribution, but is characterised in any realistic case by a strong oscillation.

3.3 Exponential term

A lateral displacement of test and basis function in the spatial domain leads to an exponential term in the spectral domain, which represents oscillating behaviour, as can be seen by Euler's theorem: $\exp(jx) = \cos(x) + j\sin(x)$. For greater distances, the oscillation become faster, resulting in a higher number of necessary sampling points for numerical integration. Hence, especially for greater distances the minimum number of sampling points is determined by the exponential term, if not a special treatment of the oscillating behaviour is done.

Eqn. 12 emphasises the different separable functions of the integral kernel of eqn. 7, using additionally $\phi_{un} = \phi_u^*\phi_n$, $\phi_{unx}(k_x) = \phi_{unx}(-k_x)$ and $\phi_{uny}(k_y) = \phi_{uny}(-k_y)$

$$\begin{aligned} K_{un} = Z_{yy} \quad & \phi_u^*\phi_n e^{j(k_x\Delta x + k_y\Delta y)} \\ = Z_{yy}(k_r, k_\phi) \quad & \phi_{unx}(k_x)\cos(k_x\Delta x) \quad (11) \\ \cdot \quad & \phi_{uny}(k_y)\cos(k_y\Delta y) \quad (12) \end{aligned}$$

4 Integration further away from the pole rings

At a greater distance from the pole ring, the Green's function is rather smooth in comparison to the other terms of the product. Thus, a product integration method [7] can be used for evaluating the integral. First the integral area is divided in several rectangular parts

$$\begin{aligned} A_{un} &= 4\int_0^{\infty}\int_0^{\infty} K_{un}dk_x dk_y \\ &= 4\sum_{i=0}^{I}\sum_{k=0}^{K}\int_{i\Delta k_x}^{(i+1)\Delta k_x}\int_{k\Delta k_y}^{(k+1)\Delta k_y} K_{un}dk_x dk_y \end{aligned} \tag{13}$$

Then Z_{yy} is interpolated by a two-dimensional polynomial of second order

$$Z_{yy}(k_x, k_y) \approx a_{ik} + b_{ik}k_x + c_{ik}k_y + d_{ik}k_x k_y \tag{14}$$

(for a_{ik}, b_{ik}, c_{ik}, d_{ik} see the Appendix (Section 9)). Over one cell $\Delta k_x \times \Delta k_y$ the integrand of eqn. 13 can be written as

$$A_{un} = 4 \sum_{i=0}^{I} \sum_{k=0}^{K} \{ a_{ik} I'_{xi} I'_{yk} + b_{ik} I''_{xi} I'_{yk} + c_{ik} I'_{xi} I''_{yk} + d_{ik} I''_{xi} I''_{yk} \} \quad (15)$$

with

$$I'_{xi} = \int_{i\Delta k_x}^{(i+1)\Delta k_x} \phi_{unx}(k_x) \cos(k_x \Delta x) dk_x \quad (16)$$

$$I''_{xi} = \int_{i\Delta k_x}^{(i+1)\Delta k_x} k_x \phi_{unx}(k_x) \cos(k_x \Delta x) dk_x \quad (17)$$

and similarly for I'_{yk} and I''_{yk}.

The quadrature areas can be enlarged with the distance to the ring of poles. As can be seen from Fig. 3, it is useful to enlarge the outer cells by a whole-numbered multiplier to avoid difficulties at the boundaries between two regions.

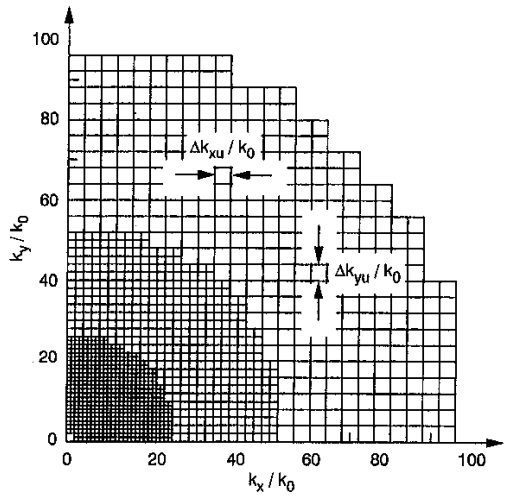

Fig.3 *Possible division of integration area into areas of different sizes*

Now the two-dimensional integral is reduced into a double sum over one-dimensional integrals. Only the rather smooth Green's function is approximated by a polynomial. The one-dimensional integrals can be evaluated numerically due to their rapidly varying behaviour. As it can be seen from eqn. 15, only K integrals for the k_x-direction and L integrals for the k_y-direction have to be solved.

The one-dimensional integrals I'_{xi}, I''_{xi}, I'_{yk}, I''_{yk} can be evaluated partly analytically by using a 'Filon-trapezoidal' rule [6, 7]. The integrals are separated into several, equidistant sections. Then only the function ϕ_{unx} is approximated by a polynomial for the numerical quadrature. The product of the polynomial and the remaining sinusoidal function is evaluated analytically. Using this procedure, it is possible to deal even with rapidly oscillating integrands, resulting in a convergence, which is almost independent of the oscillating period. The 'Filon-trapezoidal' rule is summarised in more detail in the Appendix (Section 9.2).

5 Integration in the vicinity of the poles

Eqn. 7 consists of at least one pole in k_r. Standard integration techniques for this part lead to severe numerical problems. To avoid numerical difficulties, the residual theorem can be used.

The radial part is integrated first. Hence, A_{un} of eqn. 7 can be written as

$$A_{un} = 4 \int_0^{\pi/2} \int_{k_{r0}}^{k_{r1}} K_{un} k_r dk_r dk_\varphi = 4 \int_0^{\pi/2} I_r dk_\varphi \quad (18)$$

If the poles $k_{rl} = p_i$ can be determined exactly, it is possible to divide the radial part into $2i + 1$ intervals

$$\begin{aligned} I_r &= \int_{k_{r0}}^{k_{r1}} K_{un} k_r dk_r \\ &= \int_{k_{r0}}^{p_0-\delta} K_{un} k_r dk_r + \sum_{i=1}^{i=I-1} \int_{p_i+\delta}^{p_{i+1}-\delta} K_{un} k_r dk_r \\ &\quad + \int_{p_I+\delta}^{k_{r1}} K_{un} k_r dk_r + \sum_{i=0}^{i=I-1} \int_{p_i-\delta}^{p_i+\delta} K_{un} k_r dk_r \end{aligned} \quad (19)$$

which reduces to

$$\begin{aligned} I_r &= \int_{k_{r0}}^{p_0-\delta} K_{un} k_r dk_r + \int_{p_0+\delta}^{k_{r1}} K_{un} k_r dk_r \\ &\quad + \int_{p_0-\delta}^{p_0+\delta} K_{un} k_r dk_r \end{aligned} \quad (20)$$

if there is only one pole.

The third term can be evaluated analytically from the residual theorem. If δ is small enough ($\delta < k_0/10000$ in practice), then

$$\lim_{\delta \to 0} \int_{p_i-\delta}^{p_i+\delta} = - \operatorname*{Res}_{k_r = p_i} (K_{un}) \quad (21)$$

is valid. The negative sign in eqn. 21 has to be used, because the integration path is in the mathematically negative direction.

Fig. 4 shows the principle of the quadrature close to the pole ring. For the boundary between the regions of polar and Cartesian quadrature, it is useful to implement triangular areas, which can be developed similarly to the rectangular ones outlined previously.

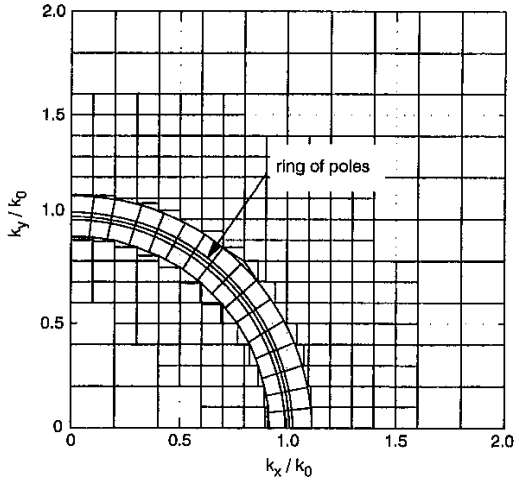

Fig.4 *Detail of quadrature area*
Quadrature has to be done in polar co-ordinates when close to the poles

6 Results

6.1 Convergence

In this Section, the proposed method is compared to a standard numerical integration. For these computations, entire domain functions for a rectangular current distribution are used. The functions consist of sinusoidal functions including an edge term [1]. The rectangular structures are 1.5mm × 1.5mm. A substrate with a height of 0.76mm and a dielectric constant of 2.35 is used. The operating frequency is 20GHz. For these types of functions, the outer regions with slow convergency are purely imaginary. Thus only the imaginary part is shown here.

Three different sizes of integration areas (Fig. 3) were used. For comparison, a polar quadrature has been implemented.

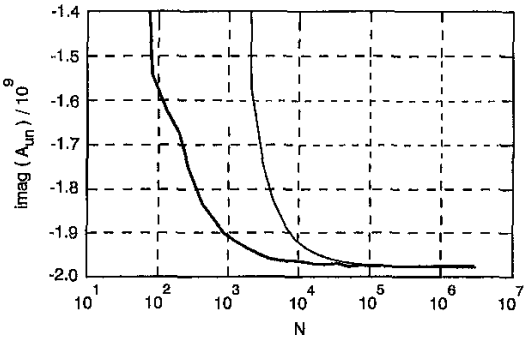

Fig.5 *Convergence of the imaginary part of the reaction integral spatial distances between test function and basis function are $\Delta x = 0$, $\Delta y = 0$*
present method
standard integration

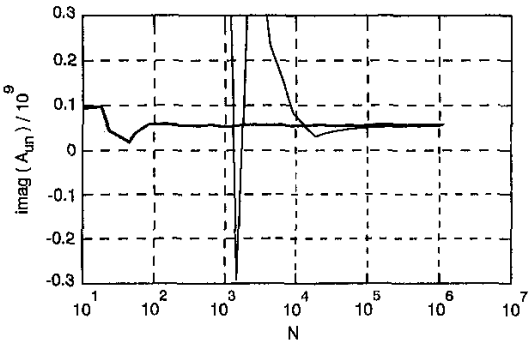

Fig.6 *Convergence of the imaginary part of the reaction integral spatial distances between test function and basis function are $\Delta x = 0.4\lambda_0$, $\Delta y = 0.4\lambda$*
present method
standard integration

In Figs. 5–7 the behaviour of the reaction integrals is shown as a function of the number of summations, in comparison to a standard trapezoidal two-dimensional polar quadrature procedure. In the standard procedure N is the number of summations terms, whereas in the method proposed here, N is the number of sums of eqn. 15. Additionally, for solving the reaction integral by our method, the integrals of eqns. 16 and 17 have to be solved. However, the numerical effort for the evaluation of these integrals can be neglected, since they are only one-dimensional. The identical number of necessary summations in the vicinity of the pole ring is not considered for both methods. The distance to the pole ring is 0.1 k_0.

Using the proposed mixed integration method, the number of summations can be decreased considerably even in the case of the self-coupling term, ($\Delta x = \Delta y = 0$, Fig. 5). Identical accuracy is achieved with only one-tenth of the summations for the standard integration method, which leads to a saving of computation time of about the same order.

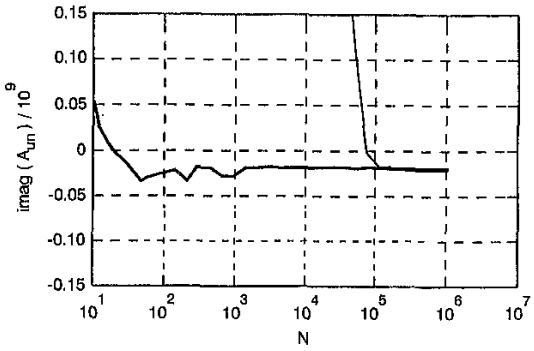

Fig.7 *Convergence of the imaginary part of the reaction integral spatial distances between test function and basis function are $\Delta x = 2\lambda_0$, $\Delta y = 0$*
present method
standard integration

In Figs. 6 and 7 the origins of the test and basis functions are at a distance of about half of the freespace wavelength and about two wavelengths, respectively. As the distance increases, the convergence of the mixed integration method improves dramatically in comparison with the standard integration method. Even for only a very small number of summations, the mixed integration method provides results very close to the actual solution. For any other method, which is not evaluating the sinusoidal functions analytically, at least a condition similar to the Nyquist theorem has to be fulfilled. Therefore, reasonable results can only be expected for a very large number of summations, resulting in considerable numerical effort.

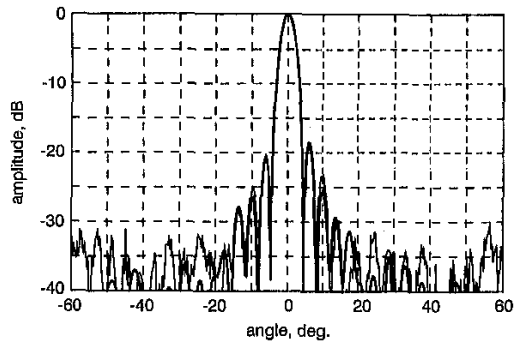

Fig.8 *E-plane pattern of a reflectarray*
theory
measurement

6.2 Example

As a very complex example for the application of the mixed integration method, the simulated and measured results of the farfield of a planar offset reflect array [8] are shown in Fig. 8. The reflectarray consists of 1117 rectangular structures. Using entire domain function with one expansion term for each patch and considering the mutual coupling of structures up to a distance of $4\lambda_0$, about 300000 integrals have to be solved numerically. With the method presented here, a computation time of less than 10 min on an HP 7000 could be achieved.

7 Conclusions

An efficient method for evaluating the reaction integrals for planar structures has been presented. The method is based on a mixed integration method, evaluating segments in Cartesian and polar co-ordinates. The algorithm can be used for current distributions, which are separable parallel to Cartesian co-ordinates. Especially for larger distances of test and basis functions the convergency is significantly better than that of the standard procedure, resulting in a high efficiency for the analysis of structures, extending even to several wavelengths.

8 References

1 TATSUO, I. (Ed.): 'Numerical techniques for microwave and millimeter-wave passive structures' (John Wiley, 1989)
2 BAILEY, M.C., and DESHPANDE, M.D.: 'Integral equation formulation of microstrip antennas', *IEEE Trans.*, 1982, **AP–30**, pp. 651–656
3 PARK, S.-O., and BALANIS, C.A.: 'Dispersion characteristics of open microstrip lines using closed-form asymptotic extraction', *IEEE Trans.*, 1997, **MTT–XX**, pp. 458–460
4 PARLEBAS, J., and WIESBECK, W.: 'Numerical methods for the full-wave analysis of coplanar elements'. Proceedings of MIOP 97, Sindelfingen, Germany, 1997, pp. 375–381
5 POZAR, D.M.: 'Improved computational efficiency for the moment method solution of printed dipoles and patches', *Electromagnetics*, 1983, **3**, pp. 299–309
6 FILON, L.N.G.: 'On a quadrature formula for trigonometric integrals', *Proc. Roy. Soc. Edinburgh*, 1928, **49**, pp. 38–47
7 DAVIS, P.J., and RADANOWITZ, P.: 'Methods of numerical integration' (Academic Press, New York, 1975)
8 PILZ, D., and MENZEL, W.: 'Analysis of a planar reflector antenna', Proceedings of Asian and Pacific *Microwave* conference, 1997, Vol. 1, pp. 225–227

9 Appendix

9.1 Approximation of the Green's function

To separate the integrand of eqn. 7 into two independent functions, the Green's function has to be approximated by a two-dimensional polynomial (eqn. 14). The function is interpolated to match the corners of one rectangle. The formulation for the coefficients is done best in matrix form

$$\vec{v}_{ik} = \frac{1}{t}\overleftrightarrow{m}\vec{f}_{ik}$$

with

$$\vec{v}_{ik} = \begin{pmatrix} a_{ik} \\ b_{ik} \\ c_{ik} \\ d_{ik} \end{pmatrix} \qquad \vec{f}_{ik} = \begin{pmatrix} f(k_{xi}, k_{yk}) \\ f(k_{xi}, k_{yk+1}) \\ f(k_{xi+1}, k_{yk}) \\ f(k_{xi+1}, k_{yk+1}) \end{pmatrix}$$

$$\overleftrightarrow{m} = \begin{pmatrix} k_{xi+1}k_{yk+1} & -k_{xi+1}k_{yk} & -k_{xi}k_{yk+1} & k_{xi}k_{yk} \\ -k_{yk+1} & k_{yk} & k_{yk+1} & -k_{yk} \\ -k_{xi+1} & k_{xi+1} & k_{xi} & -k_{xi} \\ 1 & -1 & -1 & 1 \end{pmatrix}$$

$$t = k_{xi}k_{yk} - k_{xi}k_{yk+1} - k_{xi+1}k_{yk} + k_{xi+1}k_{yk+1}$$

9.2 The Filon rule

For an integrand consisting of a product of two functions, one of which is an oscillating term of a known period, the Filon rule can be used. Only the term, which is not oscillating, is approximated by a polynomial for the sampling distance. Here, the Filon rule can be applied as follows: I_{xi} can be written with eqn. 16

$$I_{xi} = \int_{i\Delta k_x}^{(i+1)\Delta k_x} \cos(k_x \Delta x)\phi_{unx}(k_x)dk_x \qquad (22)$$

The interval is separated into several, equidistant sections

$$I'_{xi} = \sum_{n=0}^{N} \int_{i\Delta k_x+nh}^{i\Delta k_x+(n+1)h} \cos(\Delta x k_x)\phi_{unx}(k_x)dk_x \qquad (23)$$

On each section the function $\phi_{unx}(k_x)$ is interpolated by a polynomial of second order $g(k_x)$ (Fig. 9). Then it is solved analytically for each sampling distance. The procedure results in the following formula for N sampling points:

$$\begin{aligned} I'_{xi} \approx \frac{1}{\Delta x^2 h}\Big\{ & \phi_0(-\cos_1 - \Delta x h \sin_0 + \cos_0) \\ & + \sum_{n=1}^{N} \phi_n(2\cos_n - \cos_{n-1} - \cos_{n+1}) \\ & + \phi_n(\cos_N + \Delta x h \sin_N - \cos_{N-1})\Big\} \end{aligned} \qquad (24)$$

With $\cos_n = \cos\{\Delta x(nhk_x + i\Delta k_x)\}$ and $\sin_n = \sin\{\Delta x(nhk_x + i\Delta k_x)\}$, respectively.

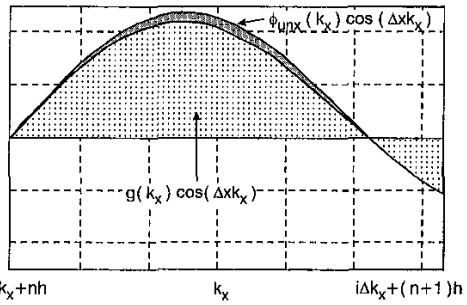

Fig.9 *Typical representation of $\phi(k_x)$ $\cos(\Delta x k_x)$ and an interpolation function in a single interval*
$g(k_x)$ is a second-order polynomial

I''_{xi} can be solved similar to I'_{xi}

$$\begin{aligned} I''_{xi} = \frac{1}{\Delta x^3 h}\Big\{ & \phi_0\big[(k_{x0} - h)\Delta x c_0 - k_{x1}\Delta c_1 \\ & - (\Delta x^2 h k_{x0} + 2)s_0 + 2s_1\big] \\ & + \sum_{n=1}^{N-1} \phi_n\big[-k_{x(n-1)}\Delta x c_{n-1} + 2k_{xn}\Delta c_n \\ & - k_{x(n+1)}\Delta c_{n+1} + 2s_{n-1} - 4s_n + 2s_{n+1}\big] \\ & + \phi_N\big[-k_{xN-1}\Delta x c_{N-1} + (x_N + h)\Delta x c_N \\ & + (\Delta x^2 h k_{xN} - 2)s_N + 2s_{N-1}\big]\Big\} \end{aligned}$$

The integrals for the y-direction can be similarly formulated.